1

Lajpat R. Ahuja

Water and Chemical Transport in the Soil Matrix and Macropores

Abstract

In this chapter, we were especially interested in simulating water flow and chemical transport through macropores explicitly, as well as in the soil matrix. For this goal, we divided the water flow process into two phases: (a) infiltration into the soil matrix and macropores and macropore–matrix interaction during a rainfall or an irrigation, modeled by using the semi-analytical, vertical and radial, Green–Ampt approach, which has been theoretically related to Richards' equation; and (b) redistribution of water in the soil matrix following infiltration, computed by a mass-conservative numerical solution of the one-dimensional Richards equation. The chemical transport during both of these phases is based on the established concept of miscible displacement but is done in a simpler way using partial piston displacement followed by partial mixing in small depth increments. Again, the Green–Ampt approach during infiltration allowed explicit transport of chemicals through macropores and explicit interaction between chemical transport through macropores and the soil matrix.

Introduction

Water flow in soil is the driving force behind all the belowground processes of an agricultural system and significantly affects aboveground plant growth and surface hydrology. It determines how much water is stored in the root zone and how much is taken up by the roots at any given time and how surface-applied fertilizers and heat are transported through this zone. All the vital microbial and biochemical transformations of organic matter and nutrients are highly dependent on soil water content and temperature. Thus, the ability of a plant to grow is also highly dependent on water

Modeling Processes and Their Interactions in Cropping Systems: Challenges for the 21st Century, First Edition. Edited by Lajpat R. Ahuja, Kurt C. Kersebaum, and Ole Wendroth.

Published 2022 by John Wiley & Sons, Inc.

flow. Furthermore, this flow largely determines how applied agricultural chemicals are transferred to surface runoff or leached below the root zone and thus how serious the impacts are on the quality of our surface and groundwater resources. This chapter is an update of Ahuja et al. (2000).

The theories of soil water movement and the related transport of chemicals and heat are now well developed for simple soil systems. One-dimensional vertical movement and retention of water in a partially or variably saturated soil profile is commonly described by a simpler form of the Richards equation that incorporates Darcy's Law and mass conservation and assumes that the role of the soil air or vapor phase and thermal gradients on the liquid flow process is negligible:

$$\frac{\partial \theta}{\partial t} = \frac{\partial}{\partial z}\left[K(h,z)\frac{\partial h}{\partial z} - K(h,z)\right] - S(z,t) \tag{1.1}$$

where θ is volumetric soil water content ($cm^3\,cm^{-3}$); t is time (h); z is soil depth (cm, assumed positive downward); h is the soil-water pressure head (cm), a function of θ; K is unsaturated hydraulic conductivity ($cm\,h^{-1}$), a function of h and z; and $S(z,t)$ is a sink term for root water uptake and tile drainage rates (h^{-1}).

Equation 1.1 can be used to described infiltration of water at the soil surface from rain or irrigation, with known rates or surface depths, and subsequent redistribution in the soil profile. For very dry portions of the soil profile, not commonly encountered in agriculture, vapor flow and the effect of soil temperatures on both liquid and vapor flow can be important. Equation 1.1 can then be modified to include these effects (Šimůnek et al., 2013). The modified equation has to be solved in conjunction with the soil heat flow equation.

The theories of chemical and heat transport in soil are based on the concept of miscible displacement of chemicals and heat by the flow of water. This concept is commonly approximated by a convection–dispersion equation. One-dimensional, miscible displacement of an absorptive and degradable chemical species through a soil column of constant water content and flux is simulated by

$$\frac{\partial}{\partial x}\left(D\frac{\partial C}{\partial x}\right) - \nu\frac{\partial C}{\partial x} - R\frac{\partial C}{\partial t} = \mu C - \gamma \tag{1.2}$$

where $C = C(x,t)$ is the chemical concentration at location x and time t; $D = \alpha_L |v|$ is the dispersion coefficient; α_L is the dispersivity; $v = q/\theta$ is the pore water velocity; θ is the volumetric water content; q is the flux density of the soil water (or the Darcy velocity); $R = 1 + \rho K_d/\theta$ is the retardation factor; ρ is the soil bulk density; K_d is the partition coefficient between solution and adsorbed phases at equilibrium; μ is the first-order decay constant; and γ is the zero-order production rate constant. For field conditions, this equation is extended to variable water contents and fluxes with space and time by solving in conjunction with the Richards equation. This equation can also be extended to nonlinear partition and nonlinear nonequilibrium or coupled sequential decay reactions (Šimůnek et al., 2013; see also Chapter 7). The heat transport equations are given in Chapter 2.

Generally for field conditions, Equations 1.1 and 1.2 have to be solved by the complex numerical methods. Simpler partially analytical approaches to these equations are available for certain conditions. However, real field soils have several complexities that play important roles which, at this stage, are not completely understood in mechanistic terms. Examples of these complexities are:

- the role of macropores—worm holes, decayed root channels, or structural cracks—in short-circuiting movement of water and chemical from soil surface to deeper layers. Šimůnek et al. (2013) approximately simulated macropore flow implicitly by an interacting dual-permeability (two-soil) system with the one-dimensional Richards equation applied to each soil.
- the role of surface aggregates in retarding downward leaching of surface-applied chemicals but increasing their transfer to runoff or to macropore flow.
- the role of interaggregate immobile pore space and chemical kinetics inside the soil matrix in retarding or enhancing transport of chemicals. This has been simulated by the Richards equation as a dual-porosity (mobile–immobile) system (Šimůnek et al., 2013).
- enormous changes in the basic soil hydraulic properties, macropores, and aggregation brought about by tillage and followed by temporal changes due to reconsolidation.
- the roles of a high water table and an installed drainage system, when incorporated in a one-dimensional model.

Most of the common cropping system models use simple sequential cascading schemes of water and chemical movement and retention in the root zone, following estimation of infiltration by a simple method such as the SCS Curve Number approach. In modeling water and chemical transport in the Root Zone Water Quality Model (RZWQM) (Ahuja et al., 2000), we utilized the existing theoretical understanding of simple soil systems but also incorporated the role of the above complexities in some simple ways, consistent with our limited knowledge of these complexities at this time. We were especially interested in simulating macropore water flow and chemical transport explicitly. For this goal, we divided the water flow process into two phases: (a) infiltration into the soil matrix and macropores and macropore–matrix interaction during a rainfall or an irrigation, modeled by using the semi-analytical, vertical and radial, Green–Ampt approach (Green & Ampt, 1911), which allows explicit flow through macropores and macropore–soil matrix interactions that the one-dimensional Richards equation does not, and has been theoretically related to the one-dimensional Richards equation (Ahuja, 1983; Morel-Seytoux & Khanji, 1974) and (b) redistribution of water in the soil matrix following infiltration, computed by a mass-conservative numerical solution of the one-dimensional Richards equation (Celia et al., 1990). Chemical transport in the soil matrix during both of these phases is based on the established concept of miscible displacement but is done in a simpler way using partial piston displacement followed by partial mixing in small depth increments. Again, the Green–Ampt approach during infiltration allowed explicit transport of chemicals through macropores and explicit interaction between chemical transport through macropores and the soil matrix.

This chapter describes the components of the model relevant to water flow and chemical transport through the soil matrix and macropores.

Description of the Soil Profile

In order to simulate the transport of water and chemicals, the soil profile must be well defined in its depth, horizon delineation, and physical and hydraulic properties. It can have either homogeneous soil properties with depth or up to a certain number of distinct soil horizons. The RZWQM uses soil horizons to define segments with like soil properties. It then creates two numerical grids, one a nonuniform layering system

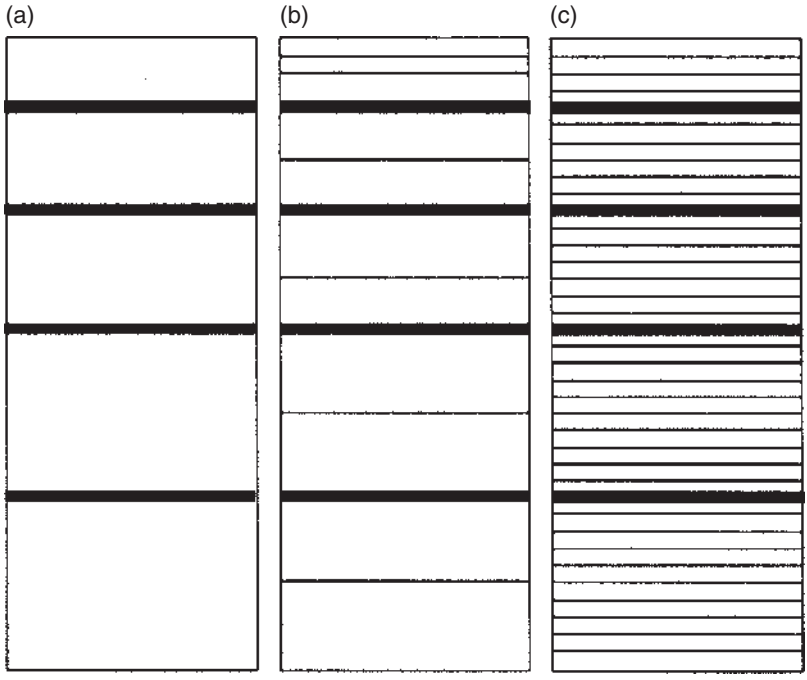

Figure 1.1 The three transport grids used by the Root Zone Water Quality Model: (a) soil profile delineated by horizons for defining hydraulic properties; (b) soil profile delineated by numerical layers for redistribution; and (c) soil profile delineated by 1-cm layers for infiltration.

for redistribution and the other a 1-cm grid used during infiltration (Figure 1.1). These grids are discussed further under Numerical Methods and Space Discretization.

Each soil horizon is characterized by its own soil physical and hydraulic properties. The physical properties are bulk density, particle density, porosity, and texture. Hydraulic properties are defined by the soil water content–matric suction relationship and the unsaturated hydraulic conductivity–matric suction relationship. These relationships are described by functional forms suggested by Brooks and Corey (1964) with slight modifications (Figure 1.2). The Brooks–Corey parameters have been compiled by Rawls et al. (1982) for 11 soil textural classes. These relationships are assumed non-hysteretic.

The soil water content versus the matric suction relationship is represented by

$$\theta(\tau) = \theta_s - A_1\tau; \qquad \tau \le \tau_b \tag{1.3}$$

$$\theta(\tau) = \theta_r + B\tau^{-\lambda}; \qquad \tau > \tau_b$$

where θ is volumetric soil water content ($cm^3\,cm^{-3}$), τ is matric suction head (cm, $\tau = |h|$, where h is the soil water pressure head), θ_s is the saturated soil water content ($cm^3\,cm^{-3}$), θ_r is the residual water content ($cm^3\,cm^{-3}$), τ_b is the air-entry or bubbling suction head (cm), λ is the pore size distribution index, and A_1, B, and λ are constants. The constant B is not an independent parameter; it is determined from other parameters by the condition of continuity at $\tau = \tau_b$. When A_1 is set equal to zero, Equation 1.3 reduces to the Brooks–Corey model.

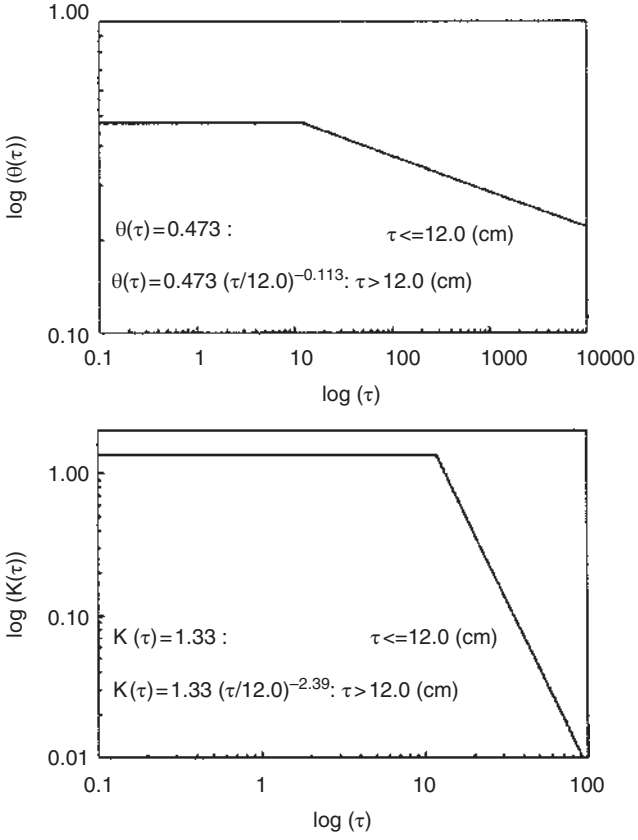

Figure 1.2 An example of the soil hydraulic property functions (soil water content–suction curve [θ–τ] and hydraulic conductivity–suction curve [*K*–τ]) used in the model. The values of the variables used in Equations 1.3–1.4 are $\theta_s = 0.473$, $A_1 = 0.0$, $\theta_r = 0.0$, $B = 0.473/(12^{-0.113})$, $\lambda = 0.113$, $\tau_b = 12.0$, $K_s = 1.33$, $N_1 = 0.0$, $K_2 = 1.33/(12^{-2.39})$, $N_2 = 2.39$, and $\tau_{bK} = 12.0$. *Source:* Based on Brooks and Corey 1964.

The hydraulic conductivity versus matric suction relation is expressed as

$$K(\tau) = K_s \tau^{-N_1}; \quad \tau \le \tau_{bK} \qquad (1.4)$$
$$K(\tau) = K_2 \tau^{-N_2}; \quad \tau > \tau_{bK}$$

where K is hydraulic conductivity (cm h^{-1}), K_s is field-saturated hydraulic conductivity (cm h^{-1}), and τ_{bK} is the air-entry or bubbling suction head for this function (cm), which may be equal to τ_b introduced above, and N_1 and N_2 are constants. In the original Brooks–Corey equation, N_1 is zero, $K_2 = K_s$, and $N_2 = 2 + 3\lambda$.

Another commonly used model of soil hydraulic properties was proposed by van Genuchten (1980). This model smooths the water retention curve near saturation:

$$\theta(h) = \frac{\theta_r + (\theta_s - \theta_r)}{(1 + |h|^n)^m}; \quad h \le 0 \qquad (1.3a)$$
$$\theta(h) = \theta_s; \quad h \ge 0$$

where h is the soil water pressure head ($-\tau$, cm), $\theta(h)$ ($cm^3\ cm^{-3}$) is the volumetric water content (for $h < 0$), θ_r ($cm^3\ cm^{-3}$) is the residual water content, θ_s ($cm^3\ cm^{-3}$) is the saturated water content, m is $1 - (1/n)$ with $n > 1$, and α (cm^{-1}) and n are empirical parameters determining the shape of the curve. Equation 1.3a smooths the water retention curve around the air-entry value.

$$K(h) = K_s S_e^l \left[1 - \left(1 - S_e^{1/m}\right)^m\right]^2 \tag{1.4a}$$

where K_s (cm h^{-1}) is saturated hydraulic conductivity and S_e is the effective saturation, expressed as $S_e = (\theta - \theta_r)/(\theta_s - \theta_r)$. The value of the exponent l in the K function is about 0.5 as an average for many soils.

Vogel and Císlerová (1988) modified the van Genuchten equations to add flexibility in the properties near saturation (higher values). Kosugi (1996) proposed a lognormal distribution model for water retention.

Estimation of Soil Hydraulic Properties

When, as often happens, measured data for these hydraulic properties are not available, they are estimated from regression equations with simpler known properties of soil texture, bulk density, and soil-water content at a 333-cm (1/3-bar) suction head ($\theta_{1/3}$). The technique can also be applied if, instead of the 333-cm value, the soil-water content at 100-cm suction is known. If neither soil-water content value is known, the parameters for the hydraulic property functions are taken from Rawls et al. (1982) based on soil texture class and adjusted based on bulk density alone.

Similar-Media Scaling

If one value of the $\theta(\tau)$ relationship is known, the rest of the function values are estimated by the extended similar-media scaling technique (Ahuja et al., 1985). According to the scaling concept (Simmons et al., 1979; Warrick et al., 1977), the matric suction for a fixed degree of saturation, S [$S = (\theta - \theta_r)/(\theta_s - \theta_r)$], at the ith site, $\tau_i(S)$, is related to the mean τ value for a soil type, $\tau_m(S)$, by

$$\alpha_i \tau_i(S) = \tau_m(S) \tag{1.5}$$

where α_i is a scaling factor for the ith site that applies at all different values of S. Therefore, if $\tau_m(S)$ is known and one value of $\tau_i(S)$ is also known, we can obtain the rest of the unknown $\tau_i(S)$ function. In our model, we utilize the textural-class mean $\theta(\tau)$ or $\tau(S)$ functions of Rawls et al. (1982) as our reference $\tau_m(S)$ functions. We also assume that the soil texture, bulk density, and the 333- or 100-cm water content at the unknown ith site are known. The value of θ_s is assumed equal to porosity, which can be calculated from the soil bulk density. Thus we can estimate the entire $\tau_i(S)$ or $\theta_i(\tau)$ function. This scaling technique is illustrated in Figure 1.3.

A different technique is used in the model to estimate changes in soil hydraulic properties due to tillage and subsequent reconsolidation. For this purpose, the change in soil bulk density is assumed to be known. The effects of tillage on soil bulk density and hydraulic properties are discussed in Chapter 11.

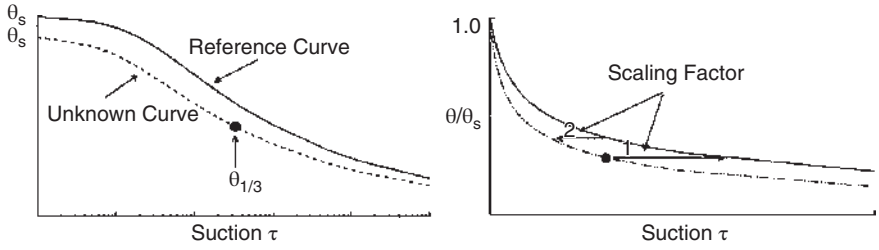

Figure 1.3 Scaling approach used to estimate the soil water content—suction relationship, θ(τ), from two known points, θ at saturation (θ_s) and θ at 333-cm suction head ($\theta_{1/3}$), and a reference curve for the soil type or textural class.

One-Parameter Model

A one-parameter model is based on the strong linear correlation ($R^2 = 0.95$) observed between the slope b and intercept a of the log–log linear $h(\theta)$ form of the Brooks–Corey equation below the air-entry value (Ahuja & Williams, 1991; Gregson et al., 1987). Furthermore, the a versus b relationship of a large group of soils merged very nicely into one common relationship $a = p + qb$, with p and q nearly constant for all soils. This allows the determination of the $h(\theta)$ function from one known value, preferably the field capacity 333-cm soil water content. This model gave good results for several soils.

The saturated hydraulic conductivity (K_s) can be user defined or estimated from the effective porosity (ϕ_e), which is defined as

$$\phi_e = \theta_s - \theta_{1/3} \tag{1.6}$$

Recent work by Ahuja et al. (1989) with nine different soils indicated that the K_s of a soil layer is strongly related to ϕ_e as

$$K_s = 764.5\phi_e^{3.29} \tag{1.7a}$$

with $R^2 = 0.67$ and RMSE of log $K_s = 0.613$

Number of data points for Equation 1.7a = 473

Fitting to the texture mean values of Rawls, et al (1982) also gave good results:

$$K_s = 509.4\phi_e^{3.633} \tag{1.7b}$$

The measurement of saturated hydraulic conductivity is normally subject to a large error (an order of magnitude) because of the unknown effects of air entrapment and the presence of macropores. Considering this limitation, Equations 1.7a and 1.7b provide a good means to estimate K_s where measured data are not available. From knowledge of K_s and $\theta(\tau)$, the complete unsaturated hydraulic conductivity function, $K(\tau)$, is obtained by utilizing the approximate capillary-bundle approach described by Campbell (1974) and others. Once soil properties are defined, modeling of flow and transport processes begins.

Vertical Infiltration of Water into the Soil Matrix

The Green–Ampt equation is used to calculate infiltration rates into a homogeneous or layered profile divided into 1-cm increments (Childs & Bybordi, 1969; Green & Ampt, 1911; Hachum & Alfaro, 1980):

$$V = \overline{K}_s \frac{\tau_c + H_o + Z_{wf}}{Z_{wf}} \tag{1.8}$$

where V is the infiltration rate at any given time (cm h^{-1}), $\overline{K}_s$ is the effective average saturated hydraulic conductivity of the wetting zone (cm h^{-1}), τ_c is the capillary drive or suction head at the wetting front (cm), H_o is the depth of surface ponding (cm), if any, and Z_{wf} is the depth of the wetting front (cm).

If the infiltration rate calculated by Equation 1.8 is greater than the rainfall rate, it is set equal to the rainfall rate (Mein & Larson, 1973). If the converse is true, the excess rainfall is considered overland flow (runoff).

For a homogeneous soil or surface of a layered soil, the effective saturated hydraulic conductivity, $\overline{K}_s$, in Equation 1.8 is set equal to the field-saturated hydraulic conductivity of the soil or horizon. For a layered soil profile with hydraulic conductivity decreasing with depth, $\overline{K}_s$ is set equal to the harmonic mean effective saturated hydraulic conductivity of the wetted zone (Childs & Bybordi, 1969; Hachum & Alfaro, 1980). Thus, for such a layered soil, the effective saturated hydraulic conductivity changes as the wetted depth increases with time. If the saturated hydraulic conductivity of a subsoil layer in a layered soil is greater than that of the layers above, the conductivity of the previous layer continues to govern the flow in this subsoil layer (Hanks & Bowers, 1962).

Based on the work of Bouwer (1969), Morel-Seytoux and Khanji (1974), and Brakensiek and Onstad (1977), it has been found that $\overline{K}_s$ in Equation 1.8 may be reduced by about half due to entrapped air and the resulting viscous resistance. Thus, the actual infiltration rate may be less than that predicted by Equation 1.8. To account for the effects of entrapped air, $\overline{K}_s$ is divided by a viscous resistance correction factor of 2.0, changing Equation 1.8 to

$$V = \frac{\overline{K}_s}{2.0} \frac{\tau_c + H_o + Z_{wf}}{Z_{wf}} \tag{1.9}$$

To account for the effects of a surface crust, an adjustment is made to the saturated hydraulic conductivity, K_s, of the first horizon. Assuming the crust is 0.5 cm thick with a known conductivity, we approximate the value of the suction head at the crust–soil interface under steady-state conditions. Then, the saturated conductivity of the first horizon is assumed to be the conductivity associated with this head value. Because infiltration is governed by the smallest K_s of the wetted soil, this adjusted value can greatly decrease infiltration. Surface crusts are destroyed by tillage and are assumed to reform immediately after rainfall.

The capillary drive, τ_c, in Equation 1.9 varies from horizon to horizon, corresponding to the location of the wetting front. It is calculated from the unsaturated hydraulic conductivity–suction function, $K(\tau)$, of the wetting horizon as (Ahuja, 1983; Swartzendruber, 1987)

$$\tau_c = \frac{\int_0^{\tau_n} K(\tau)\,d\tau}{K_s} \tag{1.10}$$

where τ_n is the suction corresponding to the average initial soil water content of the soil horizon. The $K(\tau)$ function can be analytically integrated to solve for τ_c.

A simple and efficient scheme is then used to obtain cumulative infiltration with time. It involves the following steps:

1. An average infiltration rate, V, is calculated by Equation 1.9 using Z_{wf} corresponding to the middle of the 1.0-cm wetting increment.
2. The moisture deficit in this increment is calculated as the difference between the known field-saturated value for the layer (taken as 0.9 or a given fraction of porosity) and the initial moisture (the initial moisture of the wetting increment can change from the original value by lateral absorption below the wetting front from macropores, if present, as described below).
3. The time step in wetting this increment of soil is defined as the deficit divided by the average infiltration rate.
4. These incremental deficits and time steps are summed, thus calculating the cumulative infiltration and time.

The time step for infiltration is thus the time required to wet the last wetting 1-cm increment. The time step increases with time.

Flow into Tile Drains During Infiltration

Movement of water and chemicals below the wetting front during infiltration is assumed to occur according to unit gradient flow except in two cases. In the case of a constant pressure head bottom boundary condition, no transport occurs below the wetting front during infiltration. Unit gradient flow is also not assumed if a water table is present, but it is replaced by a different algorithm, discussed below. In all other cases, however, water contents and chemical concentrations below the current depth of wetting are updated according to the hydraulic conductivity of each 1-cm increment at the end of each time step. This allows for some redistribution to occur during rainfall events and results in a small amount of leakage below the lower boundary of the profile.

When a water table is present in the soil profile above the depth of tile drains, a flux out of the drain will occur. The drainage rate is calculated from soil conditions just prior to infiltration according to the Hooghoudt equation (as outlined below). In addition, if a positive leakage rate out the bottom of the profile exists, seepage from the water table will also occur. The water that flows to the drain and out the bottom of the profile at each infiltration time step is taken from the 1-cm layer at which the water table begins, with the requirement that this layer remain above the water content at 100-cm suction (Figure 1.4). If it should fall below this water content, the water table is moved down 1 cm and the water is taken from the next 1-cm layer. If the water table falls below the tile drain, no more drainage will occur during the infiltration event, although seepage will continue.

On the other hand, if the wetting front should catch up to the water table, completely saturating the profile, the rainfall event continues by taking time steps of five minutes.

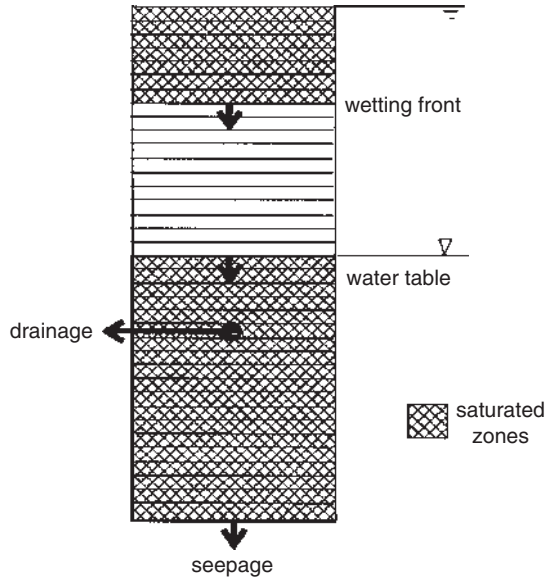

Figure 1.4 Movement of water during infiltration. The wetting front moves down in 1-cm increments as each 1 cm becomes saturated. The water table likewise moves down as water from the top of the water table is moved through the profile into drainage and/or seepage.

A new drainage rate is calculated based on the new depth of the water table, assumed to be at the surface. Then rainfall infiltrates at the drainage plus leakage rates, with any excess going into runoff. If the rainfall rate is such that it cannot satisfy drainage demands, the soil surface layers can become desaturated, and the water table will move back down.

Transport of a Chemical Within the Soil Matrix during Infiltration

We use a sequential partial-displacement and mixing approach in 1-cm increments to transport solutes in the spirit of the established phenomenon of the miscible displacement. However, the soil matrix is subdivided into micropore (immobile) and mesopore (mobile) zones, which introduces a form of preferential chemical transport in the soil matrix (the preferential flow in macropore channels outside the soil matrix is treated separately). The soil matrix porosity is divided into meso- and micropores based on either the user input values of these or the partitioning of the soil water retention curve at an arbitrary suction of 2,000 cm (Addiscott, 1977). Initially and during first wetting of a 1-cm depth increment, the water and chemicals in meso- and micropores are in equilibrium. During successive infiltration steps, the miscible displacement of solution in the saturated soil layers occurs only in the mesopores (mobile regions). This approach is similar to the layer model of Addiscott (1977), but the method of displacement involves only partial piston displacement as described below.

For each infiltration step, the soil solution is partially displaced sequentially across the 1-cm soil increments in the manner of piston displacement, followed by mixing in

each increment. To simulate this partial displacement, we assume a two-stage process. In the first stage, half of the volumetric air space of the wetting increment is filled. Soil solution is displaced through the mesopores of the wetted increments by this amount and mixed before the second displacement step is taken. The second step then moves the remaining water and its solution through the mesopores of the wetted profile in the same manner. This two-stage process simulates miscible displacement and dispersion in the mesopores. In soils that are initially very dry and in which the dispersion is low, we have obtained better results with a one-stage displacement, but the two-stage process works well in most cases and no changes are needed in the program.

The model allows diffusion between meso- and micropore solutions for certain chemicals applied by the user, such as pesticides or tracers. The equation for this process is

$$\frac{\Delta C_{sol}}{\Delta t} = D_a (C_{micr} - C_{sol}) \tag{1.11}$$

where C_{sol} is the concentration of chemical in solution (mg L^{-1}) in the mesopores, C_{micr} is the concentration in solution of the micropores (mg L^{-1}), and D_a is the apparent diffusion coefficient or diffusion distance factor (user defined or calculated from a default database).

At the end of each time step, the exchange of chemical is calculated and the concentrations in each 1-cm increment appropriately adjusted.

For a soil-adsorbed chemical, such as some pesticides, a linear relationship and an instantaneous equilibrium are assumed to occur between the soil solution and adsorbed phases in both meso- and micropore regions. We also have an option in the model to allow a portion of a reactive chemical in the soil matrix to be subject to a first-order kinetic absorption–desorption between solid and solution phases. The equations for these processes are (Cameron & Klute, 1977)

$$C_{ad} = f K_d C_{sol} \tag{1.12}$$

$$\frac{\Delta C_{ab}}{\Delta t} = R_{Kz}[(1-f) K_d C_{sol} - C_{ab}] \tag{1.13}$$

where C_{ad} is the concentration of chemical on the soil surface (g g^{-1}) in equilibrium with the solution phase, C_{sol} is the concentration in the soil solution (mg L^{-1}), f is the fraction of sorption sites of soil in equilibrium, K_d is the partition coefficient between C_{sol} and C_{ad}, C_{ab} is the concentration in the solid phase (g g^{-1}) not in instantaneous equilibrium (kinetic pool), t is time, and R_{Kz} is a kinetic rate constant.

The parameters needed for the processes are either user supplied for each chemical or obtained from a default empirical database.

At the end of an infiltration event, when the water movement slows down, the meso- and micropore regions are allowed to equilibrate and the overall solute concentration is calculated. However, instantaneous equilibrium and kinetic pools are kept separate for redistribution.

If the water table is present, the flux within the water table will carry chemicals with it that may go out through the drain and into seepage. The transport of chemicals in this saturated zone is calculated using piston displacement in only the mesopores, similar to the method described below. After the initial infiltration and chemical transport into the soil matrix has occurred within a time step, the flux of water from the top of the water table to the bottom of the profile is displaced sequentially across the 1-cm increments, mixing with the chemical concentration in the mesopores of each increment. At the depth of the tile drain, the new mesopore chemical concentration is the

concentration in the drainage water. Similarly, the concentration of chemicals in the seepage water is equal to the concentration in the mesopores in the bottom layer of the profile. To simplify the processes in the water table, two-stage displacement, diffusion between micro- and mesopores, and kinetic absorption–desorption processes are not simulated. The meso- and micropore regions below the water table are allowed to equilibrate at the end of the infiltration event.

Transfer of the Chemical to Overland Flow during Rainfall

Overland flow (also referred to as runoff) is calculated as the difference between the rainfall and infiltration in each time step. The model does not currently simulate the storage of runoff, but instead, in the absence of macropores, considers this water and its chemical solution as a loss to the system. The chemical in overland flow is extracted from the soil surface layers by raindrop impact. The extraction occurs from depths as great as 2 cm, but the contribution decreases exponentially with depth (Ahuja, 1986). This process can be modeled as an accelerated diffusion (Ahuja, 1990), but here we use a simpler approximation. We model this extraction process with a nonuniform mixing model (Ahuja, 1986; Heathman et al., 1986). The degree of mixing (M) between rainwater and soil solution in the micro- and mesopores is assumed to be complete (equal to unity) at the soil surface ($z = 0$ cm) and to decrease with depth as

$$M = \exp(-bz) \tag{1.14}$$

where b is a parameter that depends somewhat on the soil type, surface roughness, and cover conditions. Equation 1.14 can be integrated over a 1-cm increment and an average value of mixing, M_{ave}, calculated. This value may then be expressed in the same functional manner as Equation 1.14 as

$$M_{ave} = \exp(-Bz) \tag{1.15}$$

where B is a new exponent, different from b, and z is the depth of the midpoint of the increment. The value of B is kept constant for both of the top two soil compartments, which, with the experimentally determined value of B as 4.4 cm^{-1} (Ahuja, 1986), gives a degree-of-mixing value in the 1–2-cm layer of approximately 1/100 of that in the top 1-cm increment. We compute chemical transfer to overland flow (then available to move into the macropores or run off the site) from micro- and mesopores by Equation 1.15 at the midpoint of the top two 1-cm intervals. During each infiltration step in which overland flow occurs, the chemical is first transferred to the rainfall solution, part of which then infiltrates into the soil. Thus, the water that infiltrates during the time interval has the same chemical concentration as the overland flow.

Transport of Overland Water and Chemical in Solution through Macropores

Two domains of flow, the soil matrix and macropore channels, interact through the walls of the macropores, which act as a common boundary condition or a source–sink term. Thus, in concept, our model is similar to the transient water flow models of Hoogmoed and Bouma (1980), Beven and Germann (1981) and Hetrick et al. (1982). However, the methods used here are different. The only source of water and chemicals transported through the macropores is the overland flow (rainfall excess) generated at

the soil surface and the chemicals it picks up from the surface soil by mixing and raindrop impact. The solution flow in macropores is assumed very rapid and unaffected by pore tortuosity. The water solution is, however, subject to lateral absorption into the drier soil matrix. The reactive chemicals in solution are also subject to adsorption to or desorption from the macropore walls. The top soil horizons are assumed to have cylindrical macropore channels, although in the bottom horizons these may be replaced with planar cracks. Continuous macropores are idealized to be vertical and well dispersed within the soil matrix continuum. The continuity extends to the groundwater table or to a point above the depth of interest. However, a certain number of dead-end macropores are assumed to branch horizontally off the continuous pores in each soil horizon. The average volume fraction of continuous and dead-end macropores and the average size of voids (radius of cylindrical macropores and width and length of cracks) are assumed to be user supplied. From this information, the number of pores or total length of cracks per unit area of soil is calculated. The maximum flow-rate capacity (K_{mac}) of the macropores is then calculated using Poiseuille's law, assuming gravity flow (unit hydraulic head gradient).

For cylindrical holes:

$$K_{mac} = \frac{N_p \rho g \pi r_p^4}{8\eta} = \frac{P_{mac} \rho g r_p^2}{8\eta} \quad \left(\text{cm h}^{-1}\right) \tag{1.16}$$

For planar cracks:

$$K_{mac} = \frac{L_c \rho g w^3}{12\eta} = \frac{P_{mac} \rho g w^2}{12\eta} \quad \left(\text{cm h}^{-1}\right) \tag{1.17}$$

where ρ is the density of water (=1.0017 g cm^{-3}), g is the gravitational constant (=1.27 × 10^{10} cm h^{-2}), r_p is the radius of cylindrical holes (cm), w is the width of planar cracks (cm), η is the dynamic viscosity of water (=36.072 g h^{-1} cm^{-1}), N_p is the number of pores per unit area, L_c is the total length of cracks per unit area (cm), and P_{mac} is the continuous macroporosity as a fraction of the soil volume.

After ponding, the water and solutes available at the soil surface are allowed to flow into continuous macropores to the limit of macropore flow capacity. For each time step, the flow is sequentially routed downward through the continuous macropores in 1-cm depth increments. In each depth increment, the macropore flow is allowed to flow into the dead-end macropores and be absorbed by the soil matrix by radial or lateral infiltration from both continuous and dead-end parts of the macropores. The dead-end macropores can also store the solution. Time-dependent lateral absorption of the solution occurs only in the drier soil matrix below the transient wetting front generated by the continuing vertical infiltration into the matrix.

This absorption is computed by radial or lateral Green–Ampt-type equations. The transient radial infiltration rate from a cylindrical macropore, V_r, is calculated as

$$V_r = \frac{2\pi K_s \tau_c}{\ln\left(r_{wf}/r_p\right)} \tag{1.18}$$

where K_s is saturated hydraulic conductivity (cm h^{-1}), τ_c is a capillary drive term for the soil matrix in the depth increment in question (cm), r_{wf} is the wetted radius at any given

time (cm), and r_p is the macropore radius (cm). The wetted radius, r_{wf}, is calculated from the quantity of water that has infiltrated.

Equation 1.18 is not applicable for the very first time step when $r_{wf} = r_p$. Then V_r is calculated as

$$V_r = 2\pi r_p \left[\frac{2K_s\tau_c(\theta_s - \theta_i)}{\Delta t_1/2}\right]^{1/2} \tag{1.19}$$

where $(\theta_s - \theta_i)$ is the initial volumetric soil water deficit in the depth increment, and Δt_1 is the first time step (h).

For planar cracks, the equation used for the lateral infiltration rate per unit length of crack is

$$V_r = \left[\frac{2\tau_c K_s(\theta_s - \theta_i)}{t}\right]^{1/2} \tag{1.20}$$

where all terms are as previously defined, and t is the cumulative time for lateral flow. Both of the above equations are constrained by an upper limit of lateral flow that depends on the initial deficit and average distance between holes or cracks.

Compaction along macropore walls may further influence the ability of the soil to absorb water and chemicals from macropores. To account for such effects, we multiplied the radial infiltration rate from the macropore by an appropriate reduction factor:

$$V_r^* = \text{SFCT} \times V_r \tag{1.21}$$

where V_r^* is the adjusted radial infiltration rate, V_r is the Green–Ampt radial infiltration rate, and SFCT is the absorption correction factor, a user-defined parameter.

Maximum absorption is achieved when the depth increment becomes saturated. The above routing continues until the available solution within a given time step is exhausted, a water table is encountered, or the lowest depth of interest is reached. Below the lowest depth, if the bottom boundary condition implies an outward flux, the remaining solution is allowed to drain away. If the bottom boundary is an impermeable layer, however, the remaining solution is added to overland flow. A record of the cumulative absorption and changing soil water content is maintained for each depth increment.

If a high water table is present, the macropores in the saturated region are assumed to be full. Thus, water moves down a macropore below the wetting front until it reaches a zone below which the soil is saturated. At that time, the remaining water may radially infiltrate into the 1-cm increments above the water table, thus raising the table and increasing the drainage flux to tiles according to Hooghoudt's equation (see below). Although this simplifying assumption ignores the radial infiltration rate by putting macropore flow directly into unsaturated increments, it allow us to simulate the macropore flow contribution to an increase in tile drainage.

Chemicals in the macropore flow are absorbed with water by the soil matrix in each depth increment. However, before water and solutes flow into the dead-end pores or

are absorbed into the soil matrix, the reactive chemicals in the available macropore flow equilibrate with the wall of the pore, resulting in either a net adsorption to the wall or desorption from the wall. This mixing and equilibration of the macropore solution with the wall occurs in the wetted zone above the wetting front, even though there is no lateral water absorption into the soil matrix in this zone. The walls of pores are assumed to consist of 0.5 mm of soil. After absorption into the soil matrix, the chemicals are uniformly mixed and equilibrated with the soil and water in the mesopores within the depth increment.

Redistribution of Water and Chemicals after Infiltration

Between rainfall or irrigation events, the soil water is redistributed by using the Richards equation:

$$\frac{\partial \theta}{\partial z} = \frac{\partial}{\partial z}\left[K(h,z)\frac{\partial h}{\partial z} - K(h,z)\right] - S(z,t) \tag{1.22}$$

where θ is volumetric soil water content ($cm^3\ cm^{-3}$), t is time (h), z is soil depth (cm, assumed positive downward), h is soil-water pressure head (cm), K is unsaturated hydraulic conductivity ($cm\ h^{-1}$), a function of h and z, and $S(z,t)$ is a sink term for root water uptake and tile drainage rates (h^{-1}).

The initial condition is given as

$$h = h(z); \quad t = 0, z \geq 0 \tag{1.23a}$$

The surface boundary condition is an evaporative flux (potential evaporation rate) until the surface pressure head falls below a minimum value (set at −20,000 cm), at which time a constant-head condition is used:

$$-K\frac{\partial h}{\partial z} + K = E; \quad z = 0, 0 < t < t_1, h(z=0) > h_{\min} \tag{1.23b}$$

$$h = h_{\min}; \quad z = 0, t > t_1$$

where E is the potential evaporation rate on the soil surface after accounting for the effect of residue cover ($cm\ h^{-1}$) and the fraction of the soil surface not shaded by the canopy (see Chapter 3), $h_{\min}$ is the minimum value of soil-water pressure head (cm), set equal to −20,000 cm, and t_1 is the time up to which E can be sustained by the soil (h).

The bottom boundary condition can be specified as a unit gradient, constant flux, or constant pressure head:

$$\frac{\partial h}{\partial z} = 0; \quad z = z_w, t > 0$$

or

$$-K\frac{\partial h}{\partial z} + K = \nu_w; \quad z = z_w, t > 0$$

or

$$h = h(z_w); \quad z = z_w, t > 0 \tag{1.23c}$$

where z_w is the lower boundary of the soil profile (cm), and ν_w is the leakage rate through the bottom of the profile (cm h^{-1}).

Before the process of redistribution begins, the chemical concentrations in solution and in the solid-phase equilibrium and kinetic pools are transformed from 1-cm depth increments to coarser and nonuniform depth increments used for computing redistribution. Thereafter, the chemicals in solution move with the Darcy flux of water from one depth increment to another, including upward movement due to evaporation. The chemical movement is done sequentially, starting from the bottom depth increment. At the end of each time step, chemical concentrations in the solution and solid phases are adjusted with respect to both the instantaneous equilibrium and kinetic pools.

Root Water Uptake

The sink term, $S(z,t)$, consists of both the distributed sink due to root uptake and a point sink arising from tile drainage. The root uptake part of the sink term, $S_r(z,t)$ (h^{-1}), is evaluated using the approach of Nimah and Hanks (1973):

$$-S_r(z,t) = \frac{[H_r + (\text{RRES} \times z) - h(z,t) - s(z,t)]R(z)K(h)}{\Delta x \Delta z} \tag{1.24}$$

where H_r is an effective root water pressure head (cm), RRES is a root resistance term and the product (RRES × z) accounts for gravity and friction loss in H_r (assumed = 1.05), $h(z,t)$ is the soil-water pressure head (cm), $s(z,t)$ is the osmotic pressure head (assumed = 0 cm), Δx is the distance from plant roots to where $h(z,t)$ is measured (assumed = 1 cm), Δz is the soil depth increment (cm), $R(z)$ is the proportion of the total root activity in the depth increment Δz as obtained from the plant growth model (could vary with t, and $K(h)$ is the hydraulic conductivity (cm h^{-1}).

The sum total of $S_r(z,t)$ throughout the root zone cannot exceed the potential transpiration demand. Equation 1.24 is solved iteratively by varying H_r until this demand is met, with the condition that H_r does not fall below h_{min}. After H_r reaches h_{min}, this value is assumed to hold steady, whereas the sum total of S_r for all depths (total root water uptake) falls below the potential demand.

Shani and Dudley (1996) used separated equations for root water uptake from the soil based on the soil water matric pressure head gradient, denoted as $S_h(z,t)$, and osmotic pressure head gradients, $S_o(z,t)$. The term for $S_h(z,t)$ still used the Nimah–Hanks equation (Equation 1.24) but without the osmotic term $s(z,t)$. The $S_o(z,t)$ term was based on the work of Maas and Hoffman (1977) as

$$-S_o(z,t) = \frac{S_{max}p(z,t)}{1 + [s(z,t)/s_o50]^3}$$

where S_{max} is the potential transpiration at t, s_o50 is the osmotic pressure head that causes a 50% yield loss, and $p(z,t)$ is a root distribution term similar to $R(z)$ in Equation 1.24.

The value of $S_r(z,t)$ was then obtained as a multiplicative function:

$$-S_r(z,t) = S_h(z,t)S_o(z,t) \tag{1.24a}$$

The integral of Equation 1.24a with respect to dz gives the total uptake from the profile at any time t. This equation gave a better simulation of the experimental data when osmotic pressure head was important (Shani & Dudley, 1996).

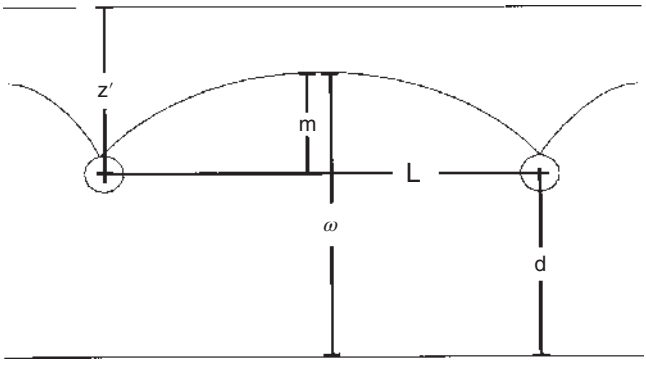

Figure 1.5 An illustration of a soil profile with a high water table and tile drains. The Root Zone Water Quality Model (RZWQM) simulates flux to the drains at the center point between the drains and reports the depth of the water table at this point. Variables represent distances used in calculating the flux to the drains in Equation 1.25.

Fluctuating Water Tables and Tile Drainage during Redistribution

If the soil profile contains a high, fluctuating water table, the depth of the water table is defined as the depth at which the pressure head first becomes non-negative and all heads below that depth are non-negative. It is allowed to fluctuate according to Equations 1.22, 1.23a, 1.23b, and 1.23c). Assuming that the pressure head value at the depth of each numerical node is known and varies linearly between nodes, the depth to the top of the water table (h = 0 cm) can be calculated.

Tile drainage is included in the term $S(z,t)$ as a point sink, $S_d(z',t)$ (h^{-1}). It is calculated from Hooghoudt's steady-state equation (Bouwer & van Schilfgaarde, 1963) as applied by Skaggs (1978). This equation is intended to correct for the two-dimensional effects of tile drainage by estimating this flux at the center point between two parallel drains, as shown in Figure 1.5. Thus, model estimates of the depth of the water table are given at the midpoint between drains. Depending on the depth of the water table, the equation for flux to the drain may be written as

$$\begin{aligned} S_d(z',t) &= \frac{8K_e d_e m + 4K_e m^2}{CL^2 \Delta z} && \omega > d \\ S_d(z',t) &= 0, && \omega \le d \end{aligned} \tag{1.25}$$

where z' is the user-supplied depth of the drain (cm), ω is the distance from the water table to the bottom of the restricting layer (cm), d is the distance from the drain to the bottom of the restricting layer (cm), m is the water table height above the drain (cm), K_e is the user-supplied or model-calculated effective lateral hydraulic conductivity (cm h^{-1}), L is the user-supplied distance between drains (cm), C is the ratio of the average flux between drains to the flux midway between drains (set = 1.0), d_e is the equivalent depth from the drain to the bottom of the restricting layer (cm), and Δz is the soil depth increment at z' (cm).

The equivalent depth, d_e, used to correct drainage fluxes in Equation 1.25 for convergence near the drain is given by (Moody, 1967)

$$d_e = \frac{d}{1 + (d/L)[(8/\pi)\ln(d/r) - \alpha]}, \quad 0 < \frac{d}{L} < 0.3$$

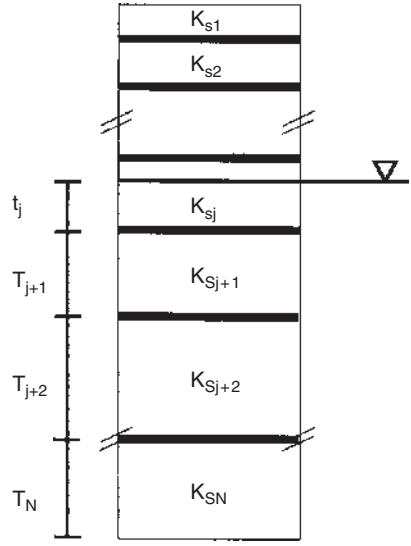

Figure 1.6 Variables used in calculating the effective saturated conductivity below the water table, where the conductivity, K_s, is defined for each horizon.

$$\alpha = 3.55 - \frac{1.6d}{L} + 2\left(\frac{d}{L}\right)^2 \tag{1.26}$$

$$d_e = \frac{L\pi}{8[\ln(L/r) - 1.15]}, \quad \frac{d}{L} \geq 0.3$$

where r is the drain tube radius (cm) and all other terms are as previously defined. This equation assumes a completely open drain tube. To account for the additional loss of head as soil water approaches real tubes, which have only a finite number of openings, an effective radius, r_e, may be used in place of the real radius, r. This is defined as the radius such that a completely open drain tube with radius r_e will offer the same resistance to inflow as a real tube with radius r (Skaggs, 1978). In general, it is slightly less than the actual radius.

Figure 1.6 depicts the variables used to calculate the effective hydraulic conductivity in the lateral direction, K_e, which is given by

$$K_e = \frac{K_{sj}t_j + \sum_{i=j+1}^{N} K_{si}T_i}{t_j + \sum_{i=j+1}^{N} T_i} \tag{1.27}$$

where K_{si} is the saturated hydraulic conductivity in the ith horizon (cm h^{-1}), T_i is the thickness of the ith horizon (cm), t_j is the depth from the water table to the bottom of the jth horizon, where the water table is in the ith horizon (cm), and N is the number of horizons.

This flux is added to the root uptake at the depth of the drain to become the sink term at that depth

$$\begin{aligned} S(z,t) &= S_r(z',t) + S_d(z',t), \quad z = z' \\ S(z,t) &= S_r(z,t), \qquad\qquad\quad z \neq z' \end{aligned} \tag{1.28}$$

Numerical Methods

Equations 1.22, 1.23a, 1.23b, and 1.23c are solved by a mass-conservative, mixed-form iterative finite-difference numerical solution (Celia et al., 1987; Celia et al., 1990). For this purpose, Equation 1.22 is written as

$$\left(\frac{1}{\Delta t}C^{n+1,m}\right)\delta^m - \frac{\partial}{\partial z}\left(K^{n+\alpha,m}\frac{\partial h^{n+1,m+1}}{\partial z}\right) = -S^n(z,t) - \frac{\partial k^{n+\alpha,m}}{\partial z} - \frac{\theta^{n+1,m}-\theta^n}{\Delta t} \tag{1.29}$$

where the superscripts n, $n+1$, and $n+\alpha$ denote the time step level (with the value of α dependent on the scheme), Δt is the time step, and m is the iteration level. The variables $C^{n+1,m}$, δ^m, and $K^{n+\alpha,m}$ are defined as

$$\begin{aligned} C^{n+1,m} &= \left.\frac{d\theta}{dh}\right|^{n+1,m} \\ \delta^m &= h^{n+1,m+1} - h^{n+1,m} \\ K^{n+\alpha,m} &= K\left(\alpha h^{n+1,m} + |1-\alpha| h^n\right) \end{aligned} \tag{1.30}$$

Equations 1.29 and 1.30 are then discretized by using either a fully implicit ($\alpha = 1$) or the Crank–Nicholson central ($\alpha = 2$) differencing scheme depending on the conditions in the soil. In soils with a high water table, we use $\alpha = 1$ and without we use $\alpha = 2$.

The initial guess of the solution of Equation 1.29 is made by taking a single Euler step (Burden & Faires, 1989, pp. 225–227):

$$\theta_i^{n+1,1} = \left\{ -K_{i-1/2}^n\left[\frac{h_i^n - h_{i-1}^n}{\frac{1}{2}\Delta z_i + \frac{1}{2}\Delta z_{i-1}}\right] + K_{i-1/2}^n + K_{i+1/2}^n\left[\frac{h_{i+1}^n - h_i^n}{\frac{1}{2}\Delta z_{i+1} + \frac{1}{2}\Delta z_i}\right] - K_{i+1/2}^n \right\}\frac{\Delta t}{\Delta z} + \theta_i^n \tag{1.31}$$

$$K_{i\pm1/2}^n = \sqrt{K\left(h_{i\pm1}^n\right) \times K\left(h_i^n\right)}$$

and then determining $h_i^{n+1,1}$ from the soil water content–matric suction relationship.

The space mesh increments increase with depth from 1.0 to 10.0 cm, according to principles outlined below and shown in Figure 1.1b. The time increment increases with time from 10^{-5} to 1.0 hours and can be set back to aid convergence of Equation 1.29 when needed. If, during any time step, the scheme should fail to converge even after setting the time step back, and the cell by cell mass balance using the current solution would be off by more than 0.5cm, the solution is set to the initial guess from Equation 1.31. This prevents erroneous solutions that may occur due to divergence of the solution. The solution of the linear system of equations at each iteration step is obtained by the Thomas algorithm.

Space Discretization

The basic principles of the space discretization are the same as described by Bresler (1973) and Ahuja and Swartzendruber (1992). For a layered soil, the placement of the space mesh increments (the numerical layers) for the numerical solution of the Richards equation must follow predetermined criteria to achieve convergence. The rules for numerical layer formation are:

- All layer thicknesses must be an integer number of centimeters; no fractions are allowed. This requires that the horizon thicknesses must also be integer numbers.

- A boundary of a numerical layer must coincide with a horizon boundary. It follows that a small adjustment may have to be made to the horizon thickness to achieve a consistent set of numerical layer boundaries and horizon boundaries.
- To satisfy the solution technique used, numerical layer boundaries are centered between solution nodes. To adhere to this rule, the distance between nodes must be odd (i.e., 1, 3, 5, 7, …) in value. This will allow layer thicknesses to remain integer values while increasing in thickness. To simulate flux boundary conditions, a fictitious node is created above the soil surface and another below the bottom of the profile.
- The first horizon must be greater than 2 cm thick.

When these rules are followed, the model will correctly move mass between the three grid systems inherent in the model. If mass imbalances appear during simulation, the grid system should be checked to ensure adherence to the numerical layer formation rules. The data-file generator program will generate correct numerical layers from horizon values.

Another factor affecting space discretization comes from the simulation of tillage. As a consequence of primary and secondary tillage, soil properties in some horizons will change. The model may create horizons in the soil profile to ensure that soil properties are changed only within the tillage zone. The depth of each type of tillage, however, varies with the instrument used. If the depth of the primary tillage is within ±1/3 of the thickness of the top soil horizon, we assume that the entire top horizon has been tilled. Otherwise, we create a new tilled horizon. The same procedure is applied for the secondary tillage. The secondary tillage generally results in creating a new horizon of its own, carved out of the original untilled or primary-tilled horizon. The depth of the secondary tilled horizon may be 2–3 cm or more depending on the implement used. When new tillage horizons are created, the numerical layers' thicknesses are adjusted to conform to the new horizon boundaries. Tillage operations are assumed to change only the soil bulk density and macroporosity, which in turn change the soil hydraulic and other properties. The decrease in soil bulk density of the tilled horizons is reversed by reconsolidation brought about by wetting and drying during subsequent rainfalls. The changes in soil physical and hydraulic properties due to tillage and reconsolidation are described in Chapter 11.

Exercises on Evaluation of the Water and Chemical Transport Model

Preferential Macropore Transport Studied with the RZWQM

The RZWQM components dealing with preferential water and chemical transport were used to study macropore flow and transport in a silty clay loam soil (Ahuja et al., 1993). Macroporosity of the soil was assumed to be 0.05% by volume, half of which was continuous and the rest discontinuous. Two rainfall sequences with two initial soil water contents, evaporation versus transpiration, macropore radius ranging from 1.0 to 0.125 mm, and three different chemicals were evaluated. During a five-weeks period, weekly rainfall of either 12.7 or 25.4 cm in one hour, with soil water redistribution and evaporation or transpiration occurring between storms, generated no macropore flow when the soil was initially dry ($h = -15{,}000$ cm). A slight amount of macropore flow was generated under the same rainfall when the soil was initially wet ($h = -330$ cm). Doubling the weekly rainfall amount and intensity generated macropore flow varying between 30 and 50% of rainfall depending on the initial and boundary conditions (Table 1.1). Chemicals transported with this flow were 0.05–8% of the

Table 1.1 Cumulative Amount of Water Entering the Macropores, Other Water Balance Components, and Amounts of Chemicals Transported in Macropores Under Different Conditions. Data for Only the Largest and Smallest Macropore Size are Presented.

Rainfall sequence–total amount for five rainfall events	Initial soil water pressure head	Upper boundary condition–evaporation (E) transpiration (T) or none (0.)[a]	Radius of macropores, if present	Flow entering the macropores (if applicable)	Runoff	Seepage below 150 cm	Actual evaporation or transpiration	Macropore flow as percent of rainfall	Amount of chemicals transported in macropores as a percent of the amount applied at the surface (40 μg/cm^2)		
									Atrazine	Prometryn	Nitrate
(cm)	(cm)		(cm)	(cm)	(cm)	(cm)	(cm)	(%)	(%)	(%)	(%)
RAIN1 12.7	−15,000	0.	–	–	0.086	0.4×10^{-4}	0.	–	–	–	–
		E	–	–	0.0	0.4×10^{-4}	6.04	–	–	–	–
		E	0.10	0.	0.	0.4×10^{-4}	6.04	0.	0.	0.	0.
		E	0.0125	0.	0.	0.4×10^{-4}	6.04	0.	0.	0.	0.
		T	–	–	0.	0.4×10^{-4}	9.44	–	–	–	–
		T	0.10	0.	0.	0.4×10^{-4}	9.44	0.	0.	0.	0.
		T	0.0125	0.	0.	0.4×10^{-4}	9.44	0.	0.	0.	0.
	−330	0.	–	–	0.421	3.24	0.	–	–	–	–
		0.	0.10	0.426	0.	3.48	0.	3.35	0.13	0.125	0.57×10^{-3}
		0.	0.0125	0.426	0.	3.48	0.	3.35	0.13	0.125	0.57×10^{-3}
		E	–	–	0.006	0.50	8.87	–	–	–	–
		E	0.10	0.006	0.	0.50	8.87	0.05	0.01	0.35×10^{-2}	0.55×10^{-3}
		E	0.0125	0.006	0.	0.50	8.87	0.05	0.01	0.35×10^{-2}	0.55×10^{-3}
		T	–	–	0.006	0.22	13.82	–	–		–
		T	0.10	0.006	0.	0.22	13.82	0.05	0.01	0.35×10^{-2}	0.55×10^{-3}
		T	0.0125	0.006	0.	0.22	13.82	0.05	0.01	0.35×10^{-2}	0.57×10^{-3}
RAIN2 25.4	−15,000	O.	–	–	9.29	$.4 \times 10^{-4}$	0.	–	–	–	–
		O.	0.0125	10.67	0.	$.4 \times 10^{-4}$	0.	42.0	3.62	3.17	0.06
		E	–	–	7.38	$.4 \times 10^{-4}$	7.67	–	–	–	–
		E	0.10	8.43	0.	$.4 \times 10^{-4}$	9.05	33.2	4.62	2.67	0.13
		E	0.0125	8.48	0.	$.4 \times 10^{-4}$	9.05	33.4	4.65	2.70	0.13
		T	–	–	6.26	$.4 \times 10^{-4}$	13.14	–	–	–	–
		T	0.10	7.71	0.	$.4 \times 10^{-4}$	13.74	30.3	2.65	2.22	0.05
		T	0.0125	7.75	0.	$.4 \times 10^{-4}$	13.74	30.5	2.67	2.25	0.05

(*continued*)

Table 1.1 (*continued*)

Rainfall sequence–total amount for five rainfall events	Initial soil water pressure head	Upper boundary condition–evaporation (E) transpiration (T) or none (0.)[a]	Radius of macropores, if present	Flow entering the macropores (if applicable)	Runoff	Seepage below 150 cm	Actual evaporation or transpiration	Macropore flow as percent of rainfall	Amount of chemicals transported in macropores as a percent of the amount applied at the surface (40 μg/cm^2)		
									Atrazine	Prometryn	Nitrate
(cm)	(cm)		(cm)	(cm)	(cm)	(cm)	(cm)	(%)	(%)	(%)	(%)
	–330	O.	–	–	11.03	4.81	0.	–	–	–	–
		O.	0.10	12.28	0.	13.61	0.	48.3	6.52	4.15	0.82
		O.	0.0125	12.33	0.	13.61	0.	48.5	6.57	4.17	0.82
		E	–	–	8.78	0.93	9.89	–	–	–	–
		E	0.10	9.97	0.	5.07	11.09	39.2	7.85	3.57	1.30
		E	0.0125	10.02	0.	5.07	11.09	39.4	7.90	3.60	1.32
		T	–	–	9.11	0.35	13.82	–	–	–	–
		T	0.10	10.88	0.	2.98	13.82	42.8	5.77	3.62	0.82

Note. Data for only the largest and smallest macropore size are presented.
[a]E, evaporation; T, transpiration; 0, none. Potential evaporation or transpiration imposed was 0.48 cm d^{-1}.

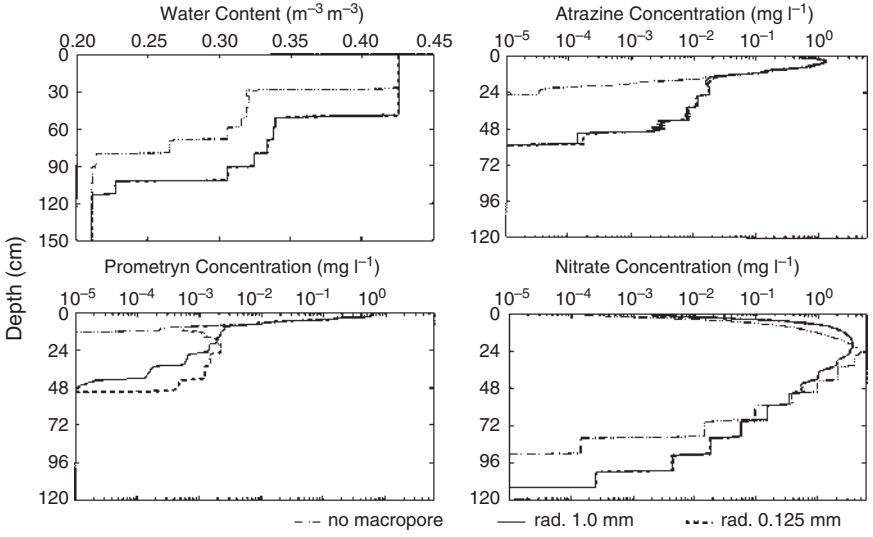

Figure 1.7 Water content and chemical concentration distributions in soil after application of 25.4 cm of rainfall, comparing results with no macropores versus macropores of two extreme sizes (1.0- and 0.125-mm radius). Initial soil water pressure head was –15,000 cm and the potential evaporation imposed at the soil surface was –4.8mm d^{-1}.

surface-applied amount, depending on conditions and the type of chemical. A moderately adsorbed chemical (atrazine) was the most susceptible to macropore transport, followed in order by a strongly adsorbed chemical (prometryn) and a mobile chemical (NO_3). The flow entering the macropores was partially absorbed by soil at progressively deeper depths; it increased the water content of the root zone and created a tail of low concentrations in the soil chemical content distributions (Figure 1.7). The macropore size had very little effect on macropore flow and transport, but the smallest size pores retarded the downward chemical movement by wall adsorption a little more than the largest size pores. Surface evaporation decreased macropore flow, soil water contents, and downward chemical movement but increased the chemical content of the macropore flow. Transpiration, on the other hand, decreased both macropore flow and its chemical content (Figure 1.8).

Macropore Transport of a Surface-Applied Bromide Tracer

This sub-model was further evaluated and refined by testing against experimental data from controlled studies in soil columns (Ahuja et al., 1995). The experiments consisted of eight treatment combinations, each in duplicate, of the following conditions: soil initially air dry versus soil initially wetted by rainfall; a 1.0-cm layer of dry aggregates on the surface versus no aggregates; and a 3-mm artificial macropore made along the column's vertical axis versus no macropore. A solution of $SrBr^2$ was atomized across the surface, followed by the application of simulated rainfall. The available data utilized were the amount of water and Br^- in surface runoff or in macropore bottom outflow (seepage), soil water content distributions, and Br^- content distributions with depth,

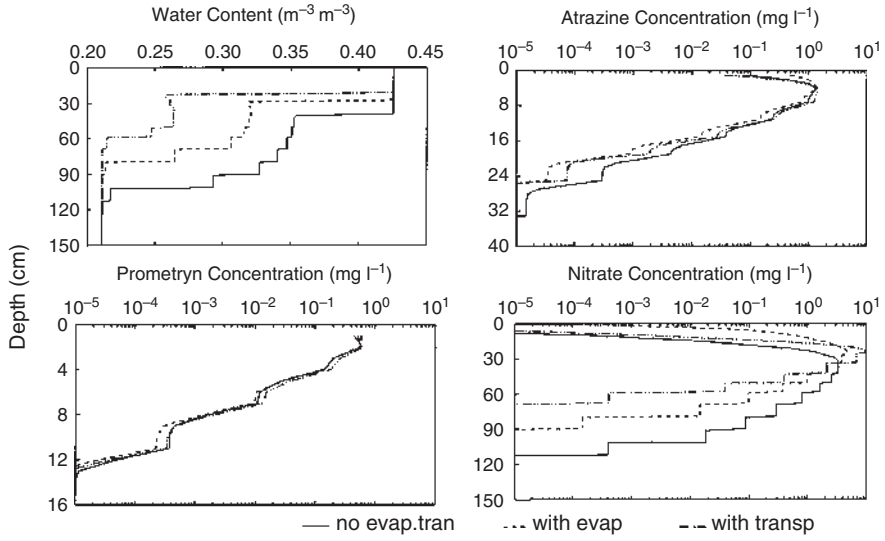

Figure 1.8 Comparison of soil moisture levels and chemical concentrations with no macropores and with and without evaporation and transpiration. Plots show conditions after application of 25.4 cm of rainfall. Initial soil water pressure head was –15,000 cm, evaporation and transpiration rates (when imposed) were –4.8 mm d^{-1}.

both above and below the main wetting front. Evaluation of the model simulations indicated that:

- The viscous resistance and entrapped air correction factor for reducing the Green–Ampt infiltration rates varied from about 2.0 for initially dry soil to about 3.0 for a prewetted soil.
- The effective lateral absorption of the macropore wall needed to be adjusted for compaction and variable water pressure around the pore circumference under small macropore flow rates.
- Better results were obtained if, in the wetted portion of the soil profile, the flow down the macropore mixed with about 0.5 mm of soil around the walls and its soil solution.
- Microporosity of surface aggregates was an important factor that held back chemical near the surface from downward leaching but kept this chemical available for mixing with rainfall, thus increasing the transfer to runoff or macropore flow.

With these refinements and calibration, the model simulations gave generally good descriptions of the data (Figures 1.9–1.14).

Other Evaluations

The sub-model has also been evaluated on field experimental data sets from the Netherlands and from Watkinsville, GA (Ahuja et al., 1996; Ma et al., 1995). For the Dutch data, the sub-model, with soil hydraulic properties estimated from bulk density and water content at $h = -333$ cm, gave good results for soil water content and Br^- distributions. For two pesticides (atrazine and metribuzine), the distributions were reasonably reproduced when the kinetic option was used with the two-site model. For the

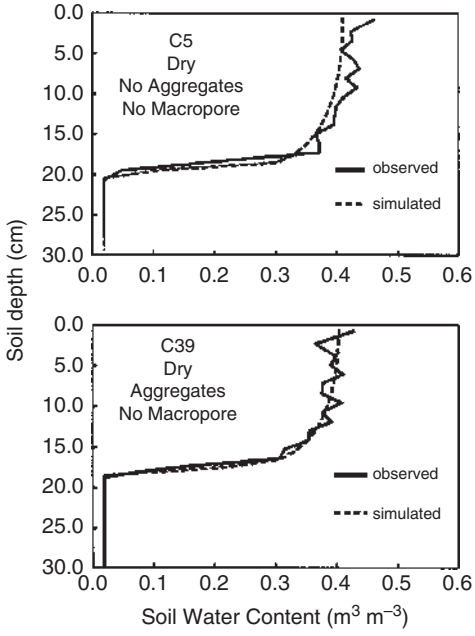

Figure 1.9 Comparison of observed and simulated soil water content distributions for initially dry columns without a macropore, with and without surface aggregates.

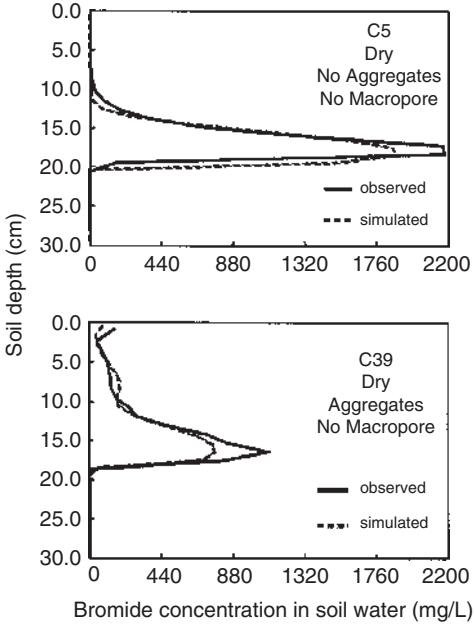

Figure 1.10 Comparison of observed and simulated soil Br^- concentration distributions for initially dry columns without a macropore, with and without surface aggregates.

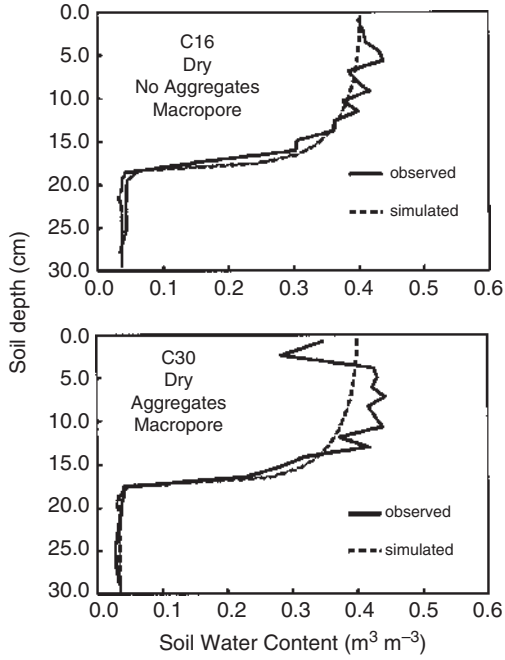

Figure 1.11 Comparison of observed and simulated soil water content distributions for initially dry columns with a macropore, with and without surface aggregates.

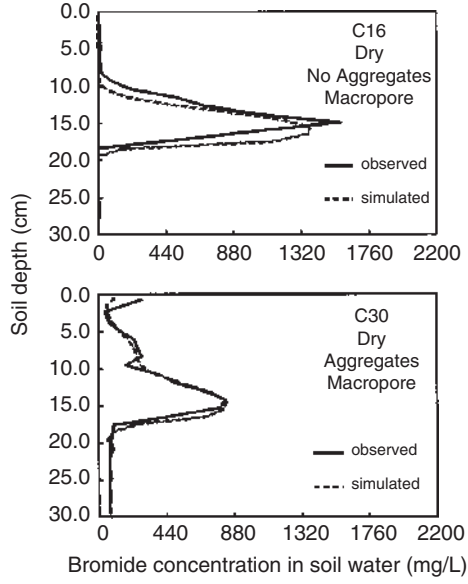

Figure 1.12 Comparison of observed and simulated soil Br^- concentration distributions for initially dry columns with a macropore, with and without surface aggregates.

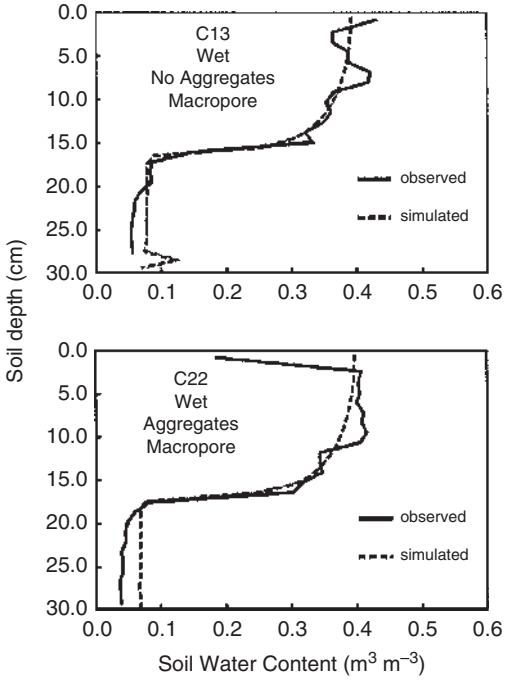

Figure 1.13 Comparison of observed and simulated soil water content distributions for initially wet columns with a macropore, with and without surface aggregates.

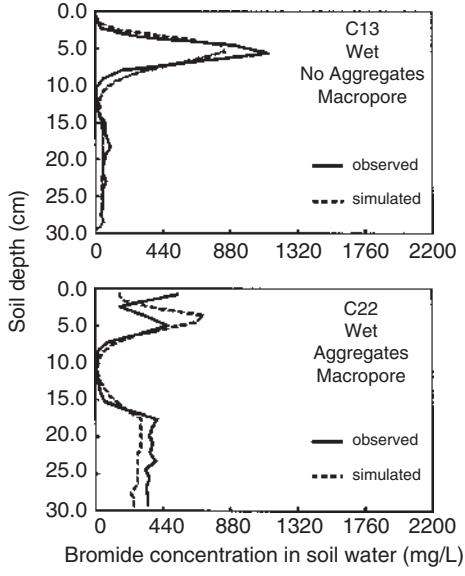

Figure 1.14 Comparison of observed and simulated soil Br^- concentration distributions for initially wet columns with a macropore, with and without surface aggregates.

Watkinsville site, the results for both soil water content and pesticides were good if a soil crust was included to match the peak runoff in one or two selected events. The pesticide concentrations in the runoff were also very well reproduced.

Using field data from the irrigation project of the Sorraia River in southern Portugal, RZWQM-simulated water content distributions during a growing season compared very favorably with observed distributions (Cameira et al., 1998). The model predicted the drying and wetting patterns seen in the top 30 cm before and after irrigations and came very close to the observed values of water content. The model also predicted very little flux below the compacted layer between 30 and 45 cm. On the same dates, predicted and observed NO_3–N concentrations were also compared. The NO_3–N concentrations were not predicted as accurately, particularly before and after the first irrigation event, but later in the season the simulated profile often came close to the range of observed values. It was demonstrated that the model did predict the downward movement of NO_3–N with water at rates comparable to those observed.

In another evaluation against soil-box data from Tifton, GA, the sub-model simulations compared very well with the experimental data for Br^- and pesticides in leaching and runoff when the kinetic option was used (Ma et al., 1996). This work demonstrated that the kinetics is extremely important in describing leaching and runoff losses from shallow soils and that the kinetics actually increased leaching of pesticides and amounts in runoff under these conditions.

Simulation of flow and transport in field soils under both dryland and irrigated corn production in eastern Colorado have further shown the ability of the RZWQM to predict these processes for a range of conditions (Buchleiter et al., 1995; Farahani et al., 1995a; 1995b, 1995c).

The tile drainage component of the RZWQM has been tested in a series of field studies in Iowa as summarized by Malone et al. (2013). The model simulated the total drainage, timing of peak flow, and seasonality fairly well. In addition, the tillage effects on tile flow were in agreement with experimental trends.

In the last two decades, extensive field testing and evaluation of the RZWQM have been done under different soil, climate, and management conditions for various applications, generally with good results. Water was the dominant factor in these studies, and the testing included parameterization of water and other important linked processes. Studies on the soil water management effects on crop water use and water quality under semiarid conditions are of special interest in this chapter (Anapalli et al., 2008, 2014, 2015a, 2015b, Bakhsh et al., 2004; Cameira et al., 2007; Hu et al., 2006; Ma et al., 2007, 2012). Recently, model use was extended to the humid conditions of the Mississippi Delta (Anapalli et al., 2016, 2018, 2021, 2019a, 2019b; Pinnamaneni et al., 2020a; 2020b; Yang et al., 2019). Guzman and Fox (2011) enhanced the RZWQM to simulate transport of soil fecal bacteria through soil macropores with good results. These studies indicate the robustness of the processes of water and chemical transport in the soil matrix and macropores described in this chapter.

Areas of Further Research

- Contribution of snow to soil water (infiltration) in conjunction with soil freezing, described in Chapter 2.
- Quantification of the effect of spatial variability of soil water properties on soil water distribution and water uptake from a field.

- Root growth distribution and its effect on water uptake distribution and on water and mass transport.
- Passive versus active plant uptake of N in conjunction with C and N and plant growth, described in the separate chapters on C and N (Chapter 5) and plant growth (Chapters 8, 9, and 10).

This chapter on soil water and chemical transport is a fundamental knowledge base that is essentially needed for advancing further research and best management in all other areas (chapters) in this book, especially for optimizing ET, transpiration and photosynthesis, surface soil and water management, climate change adaptations, heat waves, and pesticides (Chapters 3, 4, 7, 8, 10, 11, and 12).

References

Addiscott, T. M. (1977). A simple computer model for leaching in structured soils. *Journal of Soil Science*, 28, 554–563.

Ahuja, L. R. (1983). Modeling infiltration into crusted soils by the Green–Ampt approach. *Soil Science Society of America Journal*, 47, 412–418. https://doi.org/10.2136/sssaj1983.03615995004700030004x

Ahuja, L. R. (1986). Characterization and modeling of chemical transfer to runoff. *Advances in Soil Science*, 4, 149–188.

Ahuja, L. R. (1990). Modeling soluble chemical transfer to runoff with rainfall impact as a diffusion process. *Soil Science Society of America Journal*, 54, 312–321. https://doi.org/10.2136/sssaj1990.03615995005400020003x

Ahuja, L. R., Cassel, D. K., Bruce, R. R., & Barnes, B. B. (1989). Evaluation of spatial distribution of hydraulic conductivity using effective porosity data. *Soil Science*, 148, 404–411.

Ahuja, L. R., DeCoursey, D. G., Barnes, B. B., & Rojas, K. W. (1993). Characteristics of macropore transport studied with the ARS Root Zone Water Quality model. *Transactions of the ASAE*, 36, 369–380.

Ahuja, L. R., Johnsen, K. E., & Heathman, G. C. (1995). Macropore transport of a surface-applied bromide tracer: Model evaluation and refinement. *Soil Science Society of America Journal*, 59, 1234–1241. https://doi.org/10.2136/sssaj1995.03615995005900050004x

Ahuja, L. R., Johnsen, K. E., & Rojas, K. W. (2000). Water and chemical transport in soil matrix and macropores. In L. R. Ahuja, K. W. Rojas, J. D. Hanson, M. J. Shaffer, & L. Ma (Eds.), *Root Zone Water Quality Model: Modeling management effects on water quality and crop production* (pp. 13–50). Water Resources Publications.

Ahuja, L. R., Ma, Q. L., Rojas, K. W., Boesten, J. T. I., & Farahani, H. J. (1996). A field test of the Root Zone Water Quality Model: Pesticide and bromide behavior. *Pesticide Science*, 48, 101–108.

Ahuja, L. R., Naney, J. W., & Williams, R. D. (1985). Estimating soil water characteristics from simpler properties or limited data. *Soil Science Society of America Journal*, 49, 1100–1105. https://doi.org/10.2136/sssaj1985.03615995004900050005x

Ahuja, L. R., & Swartzendruber, D. (1992). Flow through crusted soils: Analytical and numerical approaches. In M. E. Sumner & B. A. Stewart (Eds.), *Soil crusting: Chemical and physical processes* (Advances in Soil Science (pp. 93–122). CRC Press.

Ahuja, L. R., & Williams, R. D. (1991). Scaling water characteristic and hydraulic conductivity based on Gregson–Hector–McGown approach. *Soil Science Society of America Journal*, 55, 308–319. https://doi.org/10.2136/sssaj1991.03615995005500020002x

Anapalli, S. S., Ahuja, L. R., Nielsen, D. C., Trout, T. J., & Ma, L. (2008). Use of crop simulation models to evaluate limited irrigation management options for corn in a semiarid environment. *Water Resources Research*, 44, W00E02. https://doi.org.10.1029/2007WR006181

Anapalli, S. S., Ahuja, L. R., Ma, L., Nielsen, D. C., Trout, T. J., Andales, A. A., Chávez, J. L., & Ham, J. (2014). Enhancing the water stress factors for simulation of corn (*Zea mays* L.) in RZWQM2. *Agronomy Journal*, 106, 81–94. https://doi.org/10.2134/agronj2013.0300

Anapalli, S. S., Ahuja, L. R., Ma, L., Trout, T. J., McMaster, G. S., Nielsen, D. C., Hamd, J. M., Andales, A. A., Halvorsone, A. D., Chávezf, J. L., & Fang, Q. X. (2015a). Developing and generalizing average corn crop water production functions across years and locations using a system model. *Agricultural Water Management*, 157, 65–77. https://doi.org/10.1016/j.agwat.2014.09.002

Anapalli, S. S., Trout, T. J., Ahuja, L. R., Ma, L., McMaster, G. S., Nielsen, D. C., Andales, A. A., Chavez, J. L., & Ham, J. (2015b). Quantification of crop water stress factors from soil water measurements in limited irrigation experiments. *Agricultural Systems*, 137, 191–205. https://doi.org/10.1016/j.agsy.2014.11.005

Anapalli, S. S., Fisher, D. K., Reddy, K. N., Krutz, J. L., Pinnamaneni, S. R., & Sui, R. (2019a). Quantifying water and CO_2 fluxes and water use efficiencies across irrigated C_3 and C_4 crops in a humid climate. *Science of the Total Environment*, 663, 338–350. https://doi.org/10.1016/j.scitotenv.2018.12.471

Anapalli, S. S., Fisher, D. K., Reddy, K. N., Rajan, N., & Pinnamaneni, S. R. (2019b). Modeling evapotranspiration for irrigation water management in a humid climate. *Agricultural Water Management*, 225, 105731. https://doi.org/10.1016/j.agwat.2019.105731

Anapalli, S. S., Fisher, D. K., Reddy, K. N., Pettigrew, W. T., Sui, R., & Ahuja, L. R. (2016). Vulnerabilities and adapting irrigated and rainfed cotton to climate change in the Lower Mississippi Delta region. *Climate*, 4, 55. https://doi.org/10.3390/cli4040055

Anapalli, S. S., Pinnamaneni, S. R., Fisher, D. K., & Reddy, K. N. (2021). Vulnerabilities of irrigated and rainfed corn to climate change in a humid climate. *Climatic Change*, 164, 5. https://doi.org/10.1007/s10584-021-02999-0

Anapalli, S. S., Reddy, K. N., & Jagadamma, S. (2018). Conservation tillage impacts and adaptations in irrigated corn (*Zea mays* L.) production in a humid climate (includes modeling). *Agronomy Journal*, 110, 2673–2686. https://doi.org/10.2134/agronj2018.03.0195

Bakhsh, A., Hatfield, J. L., Kanwar, R. S., Ma, L., & Ahuja, L. R. (2004). Simulating nitrate drainage losses from a Walnut Creek Watershed field. *Journal of Environmental Quality*, 33, 114–123. https://doi.org/10.2134/jeq2004.1140

Beven, K. J., & Germann, P. (1981). Water flow in soil macropores: II. A combined flow model. *Journal of Soil Science*, 32, 15–29.

Bouwer, H. (1969). Infiltration of water into a nonuniform soil. *Journal of the Irrigation and Drainage Division, American Society of Civil Engineers*, 95(IR4), 451–462. https://doi.org/10.1061/JRCEA4.0000669

Bouwer, H., & van Schilfgaarde, J. (1963). Simplified method of predicting the fall of water table in drained land. *Transactions of the ASAE*, 6(288–291), 296. https://doi.org.10.13031/2013.40893

Brakensiek, D. L., & Onstad, C. A. (1977). Parameter estimation of the Green and Ampt infiltration equation. *Water Resources Research*, 13, 1009–1012.

Bresler, E. (1973). Simultaneous transport of solutes and water under transient unsaturated flow conditions. *Water Resources Research*, 9, 975–986.

Brooks, R. H., & Corey, A. T. (1964). *Hydraulic properties of porous media* (Hydrology paper 3). Colorado State University.

Buchleiter, G. W., Farahani, H. J., & Ahuja, L. R. (1995). Model evaluation of ground water contamination under center pivot irrigated corn in eastern Colorado. In C. Heatwole (Ed.), *Proceedings of the International Symposium on Water Quality Modeling, Orlando, FL* (pp. 41–50). American Society of Agricultural Engineers.

Burden, R. L., & Faires, J. D. (1989). *Numerical analysis* (4th ed.). PWS-Kent Publishing Company.

Cameira, M. R., Fernando, R. M., Ahuja, L. R., & Ma, L. (2007). Using RZWQM to simulate the fate of nitrogen in field soil–crop environment in the Mediterranean region. *Agricultural Water Management*, 90, 121–136. https://doi.org/10.1016/j.agwat.2007.03.002

Cameira, M. R., Sousa, P. L., Farahani, H. J., Ahuja, L. R., & Pereira, L. S. (1998). Simulation of water and nitrate movement under fertigation applied to level-basins. *European Journal of Agricultural Engineers*, 69, 331–341.

Cameron, D. R., & Klute, A. (1977). Convective–dispersive solute transport with a combined equilibrium and kinetic adsorption model. *Water Resources Research*, 13, 183–188.

Campbell, G. S. (1974). A simple method for determining unsaturated conductivity from moisture retention data. *Soil Science*, 117, 311–314.

Celia, M. A., Ahuja, L. R., & Pinder, G. F. (1987). Orthogonal collocation and alternating-direction procedures for unsaturated flow problems. *Advances in Water Resources*, 10, 178–187.

Celia, M. A., Bouloutaas, E. T., & Zarba, R. L. (1990). A general mass-conservative numerical solution for the unsaturated flow equation. *Water Resources Research*, 26, 1483–1496.

Childs, E. C., & Bybordi, M. (1969). The vertical movement of water in a stratified porous material. *Water Resources Research*, 5, 446–459.

Farahani, H. J., Ahuja, L. R., Buchleiter, G. W., & Peterson, G. A. (1995a). Mathematical modelling of irrigated and dryland corn production in eastern Colorado. In *Clean water–clean environment–21st century: Team Agriculture working to protect water resources: Conference proceedings, Kansas City, MO* (pp. 97–100). American Society of Agricultural Engineers.

Farahani, H. J., Ahuja, L. R., Peterson, G. A., Buchleiter, G. W., & Sherrod, L. A. (1995b). Modelling of dryland and irrigated corn production systems in eastern Colorado. In *Proceeding of the Workshop on Computer Applications in Water Management, Fort Collins, CO*. Fort Collins, CO: Great Plains Agricultural Council.

Farahani, H. J., Ahuja, L. R., Peterson, G. A., Sherrod, L. A., & Mrabet, R. (1995c). Root Zone Water Quality Model evaluation of dryland/no-till crop production in eastern Colorado. In C. Heatwole (Ed.), *Proceedings of the International Symposium on Water Quality Modeling, Orlando, FL* (pp. 11–20). American Society of Agricultural Engineers.

Green, W. H., & Ampt, G. A. (1911). Studies on soil physics: 1. Flow of air and water through soils. *The Journal of Agricultural Science*, 4, 1–24. https://doi.org/10.1017/S0021859600001441

Gregson, K., Hector, D. J., & McGowan, M. (1987). A one-parameter model for the soil water characteristic. *European Journal of Soil Science*, 38, 483–486. https://doi.org/10.1111/j.1365-2389.1987.tb02283.x

Guzman, J. A., & Fox, G. A. (2011). Implementation of biopore and soil fecal bacteria fate and transport routines in the Root Zone Water Quality Model (RZWQM). *Transactions of the ASABE*, 55, 73–84.

Hachum, A. Y., & Alfaro, J. F. (1980). Rain infiltration into layered soils: Prediction. *Journal of the Irrigation and Drainage Division, American Society of Civil Engineers*, 106, 311–321.

Hanks, R. J., & Bowers, S. A. (1962). Numerical solution of the moisture flow equation for infiltration into layered soils. *Soil Science Society of America Proceedings*, 26, 530–534. https://doi.org/10.2136/sssaj1962.03615995002600060007x

Heathman, G. C., Ahuja, L. R., & Baker, J. L. (1986). Test of a non-uniform mixing model for transfer of herbicides to surface runoff. *Transactions of the ASAE*, 39(450–455), 461.

Hetrick, D. M., Holdeman, J. T., & Luxmoore, R. J. (1982). *AGTEHM: Documentation of modifications to Terrestrial Ecosystem Hydrology Model (TEHM) for agricultural applications (ORNL/TM-7856)*. Oak Ridge National Laboratory.

Hoogmoed, W. B., & Bouma, J. (1980). A simulation model for predicting infiltration into cracked clay soil. *Soil Science Society of America Journal*, 44, 458–461. https://doi.org/10.2136/sssaj1980.03615995004400030003x

Hu, C., Saseendran, S. A., Green, T. R., Ma, L., Li, X., & Ahuja, L. R. (2006). Evaluating nitrogen and water management in a double-cropping system using RZWQM. *Vadose Zone Journal*, 5, 493–505. https://doi.org/10.2136/vzj2005.0004

Kosugi, K. (1996). Lognormal distribution model for unsaturated soil hydraulic properties. *Water Resources Research*, 32, 2697–2703.

Ma, L., Ahuja, L. R., Nolan, B. T., Malone, R. W., Trout, T. J., & Qi, Z. (2012). Root Zone Water Quality Model (RZWQM2): Model use, calibration and validation. *Transactions of the ASABE*, 55, 1425–1446.

Ma, L., Malone, R. W., Heilman, P., Karlen, D. L., Kanwar, R. S., Cambardella, C. A., Saseendran, S. A., & Ahuja, L. R. (2007). RZWQM simulation of long-term crop production, water and nitrogen balances in northeast Iowa. *Geoderma*, 140, 247–259.

Ma, Q., Ahuja, L. R., Rojas, K. W., Ferreira, V. F., & DeCoursey, D. G. (1995). Measured and RZWQM predicted atrazine movement in a field soil. *Transactions of the ASAE*, 38, 471–479.

Ma, Q., Ahuja, L. R., Wauchope, R. D., Johnsen, K. E., & Burgoa, B. (1996). Comparison of instantaneous equilibrium and equilibrium–kinetic sorption models for simultaneous leaching and runoff of pesticides. *Soil Science*, 161, 646–655.

Maas, E. V., & Hoffman, G. J. (1977). Crop salt tolerance: Current assessment. *Journal of the Irrigation and Drainage Division of the American Society of Civil Engineers*, 103, 115–134.

Malone, R. W., Logsdon, S., Shipitalo, M. J., Weatherington-Rice, J., Ahuja, L., & Ma, L. (2013). Tillage effect of macroporosity and herbicide transport in percolate. *Geoderma*, 116, 191–216. https://doi.org/10.1016/S0016-7061(03)00101-0

Mein, R. H., & Larson, C. L. (1973). Modeling infiltration during a steady rain. *Water Resources Research*, 9, 384–394.

Moody, W. T. (1967). Nonlinear differential equation of drain spacing. *Journal of the Irrigation and Drainage Division, American Society of Civil Engineers*, 92(IR2), 1–10. https://doi.org/10.1061/JRCEA4.0000420

Morel-Seytoux, H. J., & Khanji, J. (1974). Derivation of an equation of infiltration. *Water Resources Research*, 10, 795–800.

Nimah, M., & Hanks, R. J. (1973). Model for estimating soil–water–plant–atmospheric interrelation: I. Description and sensitivity. *Soil Science Society of America Proceedings*, 37, 522–527. https://doi.org/10.2136/sssaj1973.03615995003700040018x

Pinnamaneni, S. R., Anapalli, S. S., Reddy, K. N., & Fisher, D. K. (2020a). Effects of irrigation and planting geometry on cotton productivity and water use efficiency. *The Journal of Cotton Science*, 24, 2–10.

Pinnamaneni, S. R., Anapalli, S. S., Reddy, K. N., Fisher, D. K., & Quintana-Ashwell, N. E. (2020b). Assessing irrigation water use efficiency and economy of twin-row soybean in the Mississippi Delta. *Agronomy Journal*, 112, 4219–4231. https://doi.org/10.1002/agj2.20321

Rawls, W. J., Brakensiek, D. L., & Saxton, K. E. (1982). Estimation of soil water properties. *Transactions of the ASAE*, 25(1316–1320), 1328.

Shani, U., & Dudley, L. M. (1996). Modeling water uptake by roots under water and salt stress: Soil-based and crop response sink terms. In Y. Waisel, A. Eshel, & U. Kafkafi (Eds.), *Plant roots: The hidden half* (2nd ed., pp. 635–641). Marcel Dekker.

Simmons, C. S., Nielsen, D. R., & Biggar, J. W. (1979). Scaling of field-measured soil water properties. *Hilgardia*, 47, 77–154.

Šimůnek, J., Šejna, M., Saito, H., Sakai, M., & van Genuchten, M. T. (2013). *The HYDRUS-1D software package for simulating the one-dimensional movement of water, heat, and multiple solutes in variably-saturated media*. Department of Environmental Sciences, University of California.

Skaggs, R. W. (1978). *A water management model for shallow water table soils* (Report no. 134). Water Resources Research Institute of the University of North Carolina.

Swartzendruber, D. (1987). Rigorous derivation and interpretation of the Green and Ampt equation. In Y. S. Fok (Ed.), *Proceedings of the International Conference on Infiltration Development and Applications* (pp. 28–37). Water Resources Research Center, University of Hawaii.

van Genuchten, M. T. (1980). A closed-form equation for predicting the hydraulic conductivity of unsaturated soils. *Soil Science Society of America Journal*, 44, 892–898. https://doi.org/10.2136/sssaj1980.03615995004400050002x

Vogel, T., & Císlerová, M. (1988). On the reliability of unsaturated hydraulic conductivity calculated from the moisture retention curve. *Transport in Porous Media*, 3, 1–15.

Warrick, A. W., Mullen, G. J., & Nielsen, D. R. (1977). Scaling field-measured soil hydraulic properties using a similar media concept. *Water Resources Research*, 13, 355–362.

Yang, W., Feng, G., Adeli, A., Kersebaum, K. C., Jenkins, J. N., & Li, P. (2019). Long-term effect of cover crop on rainwater balance components and use efficiency in no-tilled and rainfed corn and soybean rotation system. *Agricultural Water Management*, 219, 27–39.